MBOC: The New Optimized Spreading Modulation
Recommended for Galileo L1 OS and GPS L1C

**GUENTER W. HEIN,
JOSE-ANGEL AVILA-
RODRÍGUEZ, STEFAN
WALLNER,**
UNIVERSITY FEDERAL
ARMED FORCES (MUNICH,
GERMANY)

**JOHN W. BETZ,
CHRIS J. HEGARTY,
JOSEPH J. RUSHANAN,
ANDREA L. KRAAY**
THE MITRE CORPORATION

ANTHONY R. PRATT
UK DEFENCE SCIENCE AND
TECHNOLOGY LABORATORY

LT SEAN LENAHAN
GPS JOINT PROGRAM
OFFICE, LOS ANGELES AFB

JOHN OWEN,
UK DEFENCE SCIENCE AND
TECHNOLOGY LABORATORY

JEAN-LUC ISSLER
CNES (FRENCH SPACE
AGENCY)

THOMAS A. STANSELL
STANSELL CONSULTING

Members of the US/EU working group celebrate their agreement on a recommended common MBOC structure for GPS and Galileo L1 civil signals: from left to right: Chris Hegarty, Tony Pratt, Jean-Luc Issler, John Owen, Jose-Angel Avila-Rodriguez, John Betz, Sean Lenahan, Stefan Wallner, and Günter Hein.

This article introduces the multiplexed binary offset carrier (MBOC) spreading modulation recently recommended by the GPS-Galileo Working Group on Interoperability and Compatibility for adoption by Europe's Galileo program for its Open Service (OS) signal at L1 frequency, and also by the United States for its modernized GPS L1 Civil (L1C) signal. The article provides information on the history, motivation, and construction of MBOC signals. It then shows various performance characteristics and summarizes their status in Galileo and GPS signal design.

On June 26, 2004, the United States of America and the European Community (EC) established the "Agreement on the Promotion, Provision and Use of Galileo and GPS Satellite-Based Navigation Systems and Related Applications" (A copy of this agreement can be found at the website of the U.S. Space-Based Positioning, Navigation, and Timing (PNT) Executive Committee through the URL address provided in reference [1] in the "Additional Resources" section near the end of this article.)

One aspect of the agreement was to adopt a common baseline signal to be transmitted in the future by Galileo and GPS civil signals at the L1 center frequency of 1575.42 MHz. Although the agreement established BOC(1,1) as the baseline for the Galileo L1 Open Service (OS) and GPS future L1C signals, it also stated that the parties shall work together toward achieving optimization of that modulation for their respective systems, within the constraints of the Agreement.

A recent joint design activity involving experts from the United States and Europe has produced a recommended optimized spreading modulation for the L1C signal and the Galileo L1 OS signal. Details of this recommendation can be found in two documents available on-line at the NAVSTAR GPS Joint Program Office (JPO) website through the URLs provided as references [2] and [3] in the Additional Resources section. The United States is willing to adopt for GPS L1C either the baseline BOC(1,1) or the recommended MBOC modulation, consistent with what is selected for Galileo L1 OS.
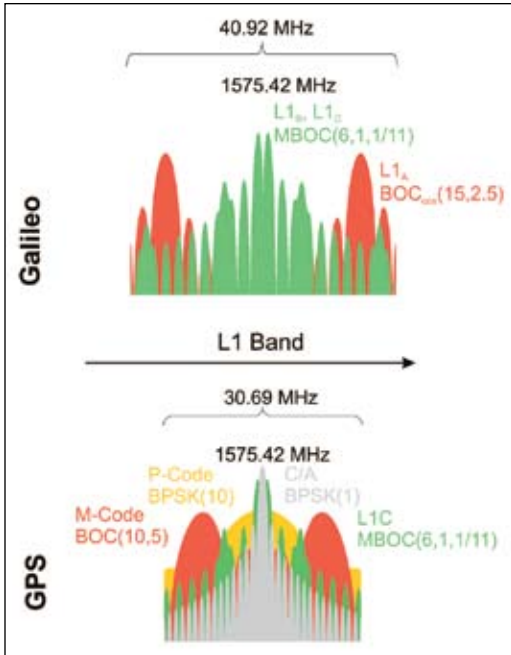
FIGURE 1. Galileo and GPS Frequency Plan with the recommended changes in GPS L1C and Galileo L1 OS

The spreading modulation design places a small amount of additional power at higher frequencies in order to improve signal tracking performance.

$$G_{Signal}(f) = \frac{10}{11} G_{BOC\,(1,1)}(f) + \frac{1}{11} G_{BOC\,(6,1)}(f) \qquad \text{(1)}$$

Figure 1 shows the resulting signal structure plan for GPS and Galileo in the L1 band that would result from the recommended changes.

This article describes the spreading modulation's power spectral density (PSD), as well as alternative spreading time series and their autocorrelation functions. In addition, it shows various measures that contrast the performance differences between the optimized modulation and other modulations. The article concludes by summarizing the status of the common spreading modulation and the way ahead.

MBOC Power Spectral Density

The spreading modulation for the legacy civil signal at 1575.42 MHz, the GPS C/A-code, is based on binary phase shift keyed (BPSK) signal with a rectangular pulse shape and a spreading code chip rate of 1.023 MHz, denoted BPSK-R(1).

Although very good performance can be obtained with the C/A code signal, it has been recognized that better performance can be obtained using spreading modulations that provide more power at high frequencies away from the center frequency.

Binary offset carrier (BOC) spreading modulations are one way to accomplish this, and under the terms of the 2004 US/EC agreement a BOC(1,1) spreading modulation was selected as the baseline for the future Galileo L1 OS and GPS L1C signals. **Figure 2** shows BOC(1,1)'s resulting increase in higher frequency power, compared to BPSK-R(1).

The multiplexed binary offset carrier (MBOC) PSD recommended in the technical working group's proposal is the PSD of the entire signal (pilot and data components together), denoted MBOC(6,1,1/11), and given by **Equation 1** in which $G_{BOC(m,n)}(f)$ is the unit-power PSD of a sine-phased BOC spreading modulation as defined in the article by J.W. Betz (2002) cited in the Additional Resources section. The selection of this PSD and identification of practical ways to produce time waveforms that implement it are based on extensive work by many individuals. Some of these foundational references can be found in the articles listed in the Additional Resources.

The resulting increase in higher frequency power MBOC(6,1,1/11), compared to that of BOC(1,1), is evident in **Figure 3**. As will be seen, the improvement in

high frequency power for signal tracking can be rendered even greater than what is shown in Figure 2 by placing all or most of the BOC(6,1) symbols, which provide the additional high frequency power, in the pilot component of the signal.

The recommended MBOC(6,1,1/11) is a specific case of more general spreading modulations that have been studied extensively. It was selected to meet technical constraints in the US/EU agreement, to retain a high degree of interoperability with receivers that might use BOC(1,1), and to facilitate implementation in satellites and receivers.

In other words, an MBOC(6,1,1/11) signal can be processed by a receiver designed for BOC(1,1). In that case, BOC(1,1) receivers can be designed to
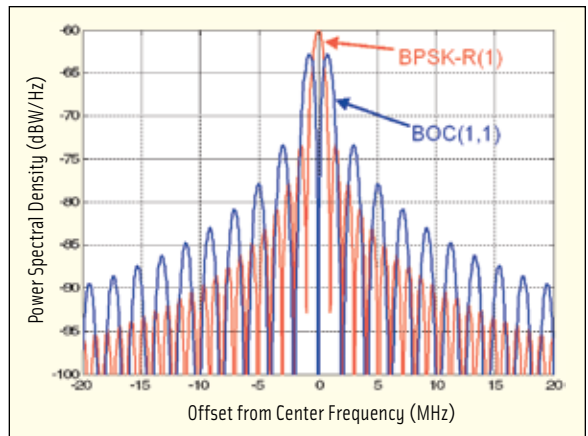

FIGURE 2. Unit Power PSDs of BPSK-R(1) and BOC(1,1) Spreading Modulations, Showing BOC(1,1)'s Additional Power at Higher Frequencies
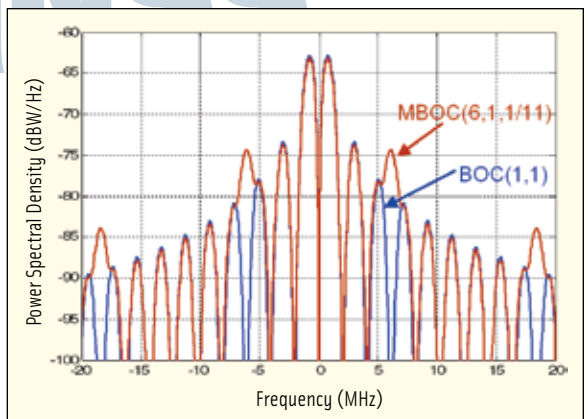

FIGURE 3. Unit Power PSDs of BOC(1,1) and MBOC(6,1,1/11) Spreading Modulations, Showing MBOC(6,1,1/11)'s Additional Power at Higher Frequencies

use only the BOC(1,1) component of the MBOC(6,1,1/11), requiring minimal or no changes to the BOC(1,1) receiver design. However, if a receiver designer wants to take advantage of BOC(6,1)'s high frequency component, the bandwidth, sampling rate, and correlation processing should be correspondingly adapted.

Spreading Time Series and Autocorrelation

A variety of time waveforms can be used to produce the MBOC(6,1,1/11) PSD described in Equation (1). In this section we will describe two different approaches, time-multiplexed BOC (TMBOC) and composite BOC (CBOC) along with various applications of each approach. Although both can produce the MBOC PSD, TMBOC and CBOC represent two fundamentally different implementations.

First, we denote a baseband spread spectrum waveform by

$$s(t) = \sum_{k=-\infty}^{\infty} a_k g_k(t - kT_c) \quad \text{(2)}$$

where the $\{a_k\}$ take on the values ±1 as determined by the combination of spreading code chip, any data message symbol, and any overlay code bit, T_c is the spreading code chip rate, and $\{g_k(t)\}$ are spreading symbols expressed in a general enough form so that they can be different for different values of k, the chip index of Equation (2).

Thus, a_k is the value of the code chip plus data message and overlay code bit, and $g_k(t)$ is the chip waveform, which in the case of TMBOC will be sometimes BOC(1,1) and other times BOC(6,1). (Clearly, more general versions of (2) could employ complex-valued $\{a_k\}$ and $g_k(t)$ to achieve higher-order phase modulations.)

Next, we define the spreading time series as the deterministic time series produced with the chip values formed by the combination of the spreading code bits, any data message symbols, and any overlay code or other secondary code. For example, a BPSK-R spreading time series takes on the constant value of unity, while a BOC time series is merely
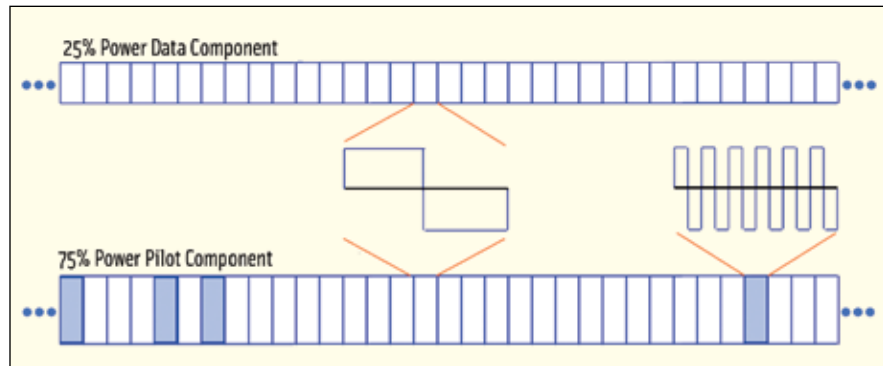

FIGURE 4. Example of TMBOC(6,1,4/33) Spreading Time Series, with All BOC(6,1) Spreading Symbols in the 75 percent Pilot Power Component

the repetition of identical BOC spreading symbols.

The most general case corresponds to BCS signals, whose time series is given by a vector s as shown in the articles by G. W. Hein et al (2005) and J. A. Avila-Rodriguez et al (2005) listed in Additional Resources. According to this the spreading time series of BPSK-R in Equation (2) is defined as

$$s(t) = \sum_{k=-\infty}^{\infty} g_k(t - kT_c) \quad \text{(3)}$$

TMBOC Implementation

In a TMBOC spreading time series, different BOC spreading symbols are used for different values of k, in either a deterministic or periodic pattern. To produce a MBOC(6,1,1/11) spectrum, the spreading symbols used are BOC(1,1) spreading symbols denoted $g_{BOC(1,1)}(t)$ and BOC(6,1) spreading symbols denoted $g_{BOC(6,1)}(t)$, with

$$g_{BOC(1,1)}(t) = \begin{cases} \text{sgn}\left[\sin(2\pi t/T_c)\right] & 0 \leq t \leq T_c \\ 0 & \text{elsewhere} \end{cases} \quad \text{(4)}$$

and defined by

$$g_{BOC(6,1)}(t) = \begin{cases} \text{sgn}\left[\sin(12\pi t/T_c)\right] & 0 \leq t \leq T_c \\ 0 & \text{elsewhere} \end{cases} \quad \text{(5)}$$

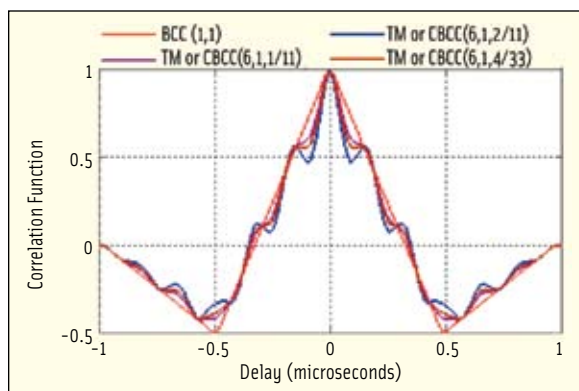Because the pilot and data components of a signal can be formed using different spreading time series, and the

FIGURE 5. Normalized Autocorrelation Functions Computed over ±15 MHz Bandwidth

total signal power can be divided differently between the pilot and data components, many different TMBOC-based implementations are possible.

A candidate TMBOC implementation for a signal with 75 percent power on the pilot component and 25 percent power on the data component could use all BOC(1,1) spreading symbols on the data component, leaving the higher frequency contributions of the BOC(6,1) for the pilot channel. Indeed, data demodulation does not benefit from the high frequency BOC(6,1) and the pilot component would have a spreading time series that comprises 29/33 BOC(1,1) spreading symbols and 4/33 BOC(6,1) spreading symbols.

This design places all of the higher frequency contributions in the pilot component, providing the greatest possible benefit to signal tracking when only the pilot channel is used for this purpose, while yielding the PSDs:

$$G_{Pilot}\left(f\right)=\frac{29}{33}G_{BOC(1,1)}\left(f\right)+\frac{4}{33}G_{BOC(6,1)}\left(f\right)$$

$$G_{Data}\left(f\right)=G_{BOC(1,1)}\left(f\right)$$

$$G_{MBOC(6,1,1/11)}\left(f\right)=\frac{3}{4}G_{Pilot}\left(f\right)+\frac{1}{4}G_{Data}\left(f\right) \qquad (6)$$

$$=\frac{10}{11}G_{BOC(1,1)}\left(f\right)+\frac{1}{11}G_{BOC(6,1)}\left(f\right)$$

Figure 4 shows an example of this implementation, with the BOC(6,1) spreading symbols in locations 1, 5, 7, and 30 of each 33 spreading symbol locations. This pattern could be repeated 310 times if the spreading code length is 10230, or 124 times if the spreading code length is 4092.

For a signal with a 50/50 power split between pilot and carrier component, a candidate TMBOC implementation would be to use all BOC(1,1) spreading symbols on the data component, and 2/11 BOC(6,1) spreading symbols on the pilot, yielding the PSDs

$$G_{Pilot}\left(f\right)=\frac{9}{11}G_{BOC(1,1)}\left(f\right)+\frac{2}{11}G_{BOC(6,1)}\left(f\right)$$

$$G_{Data}\left(f\right)=G_{BOC(1,1)}\left(f\right)$$

$$G_{MBOC(6,1,1/11)}\left(f\right)=\frac{1}{2}G_{Pilot}\left(f\right)+\frac{1}{2}G_{Data}\left(f\right) \qquad (7)$$

$$=\frac{10}{11}G_{BOC(1,1)}\left(f\right)+\frac{1}{11}G_{BOC(6,1)}\left(f\right)$$

Yet another option for a signal with 50/50 power split between pilot and carrier component would be to place 1/11 BOC(1,1) spreading symbols on both the pilot and data, yielding the PSDs

$$G_{Pilot}\left(f\right)=\frac{10}{11}G_{BOC(1,1)}\left(f\right)+\frac{1}{11}G_{BOC(6,1)}\left(f\right)$$

$$G_{Data}\left(f\right)=\frac{10}{11}G_{BOC(1,1)}\left(f\right)+\frac{1}{11}G_{BOC(6,1)}\left(f\right)$$

$$G_{MBOC(6,1,1/11)}\left(f\right)=\frac{1}{2}G_{Pilot}\left(f\right)+\frac{1}{2}G_{Data}\left(f\right) \qquad (8)$$

$$=\frac{10}{11}G_{BOC(1,1)}\left(f\right)+\frac{1}{11}G_{BOC(6,1)}\left(f\right)$$

Several considerations affect the choice of specific locations for the BOC(6,1) spreading symbols. If BOC(6,1) symbols are placed in both the pilot and data components, receiver implementation is simplest when these symbols are placed in the same locations in both components. Also, proper placement of the BOC(6,1) symbols can lead to improvement of the spreading codes' autocorrelation and crosscorrelation properties, compared to these properties with all BOC(1,1) spreading symbols.

Work is under way to determine the best placement of BOC(6,1) symbols in a L1 OS signal, accounting for these considerations. Good results have been obtained for L1C using the BOC(6,1) locations shown in Figure 3, and the resulting performance of spreading codes for L1C are reported later in this article.

CBOC Implementation

A CBOC implementation can be based on the approach presented in the articles by G. W. Hein et al (2005), J. A. Avila-Rodriguez et al (2005), and A. R. Pratt et al (2003) and (2006) listed in Additional Resources, using four-level spreading symbols formed by the weighted sum of $g_{BOC(1,1)}(t)$ and $g_{BOC(6,1)}(t)$ symbols. For a 50/50 power split between data and pilot components, CBOC symbols formed from the sum of $\sqrt{10/11}\ g_{BOC(1,1)}(t)$ symbols and $\sqrt{1/11}\ g_{BOC(6,1)}(t)$ symbols could be used on both components, yielding the PSDs in Equation (8).

Alternatively, for the same 50/50 power split between data and pilot components, CBOC symbols formed from the sum of $\sqrt{9/11}\ g_{BOC(1,1)}(t)$ symbols and $\sqrt{2/11}\ g_{BOC(6,1)}(t)$ symbols could be used on only the pilot component, with the data component remaining all $g_{BOC(1,1)}(t)$. The resulting PSDs would be the same as (7).

Table 1. MBOC(6,1,1/11) Possible implementations		
Data	Pilot	Percentage on pilot
BOC(1,1)	TMBOC(6,1,2/11)	50%
BOC(1,1)	TMBOC(6,1,4/33)	75%
TMBOC(6,1,1/11)	TMBOC(6,1,1/11)	50%
TMBOC(6,1,1/11)	TMBOC(6,1,1/11)	75%
BOC(1,1)	CBOC(6,1,2/11)	50%
BOC(1,1)	CBOC(6,1,4/33)	75%
CBOC(6,1,1/11)	CBOC(6,1,1/11)	50%
CBOC(6,1,1/11)	CBOC(6,1,1/11)	75%

The normalized autocorrelation function of the TM or CBOC(6,1,4/33) spread spectrum time series, computed over infinite bandwidth and with ideal spreading codes, is illustrated in **Figure 5**, along with the autocorrelation function for BOC(1,1). Observe that TM or CBOC(6,1,4/33)'s correlation function peak is narrower than that of BOC(1,1), but the widths at values of 0.5 and at the zero crossing are virtually the same.

Table 1 summaries the variety of implementations of MBOC(6,1,1/11) that have been outlined.

Many different performance characteristics have been considered during waveform optimization. The primary objective has been to improve tracking performance in multipath. In addition to this factor, we have also considered other characteristics, including code tracking, initial synchronization for acquisition, spreading code performance, and losses for narrowband receivers.

Multipath Performance

Because performance in multipath involves a combination of signal design and receiver processing, we have considered several different processing approaches. Furthermore, given that new ideas for multipath mitigation processing are emerging, we also considered signal characteristics that appear to benefit these advanced multipath mitigation techniques.

Multipath Performance with Noncoherent Early–Late Processing. We base our evaluation of early-late processing performance on a static model with
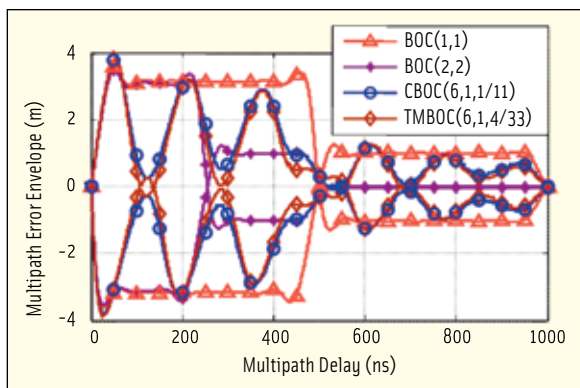
FIGURE 6. Multipath Error Envelope for NELP Processing, BW=24 MHz (4 pole Butterworth), $\Delta\tau$=24.4 nsec
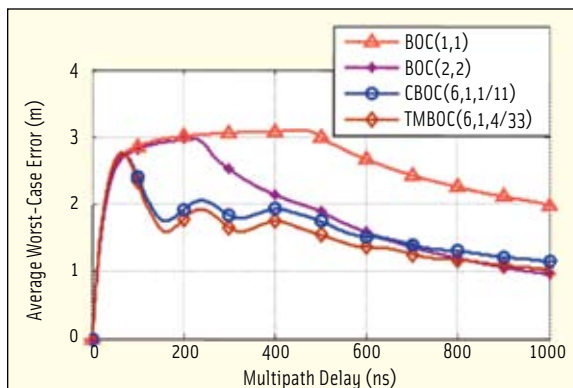

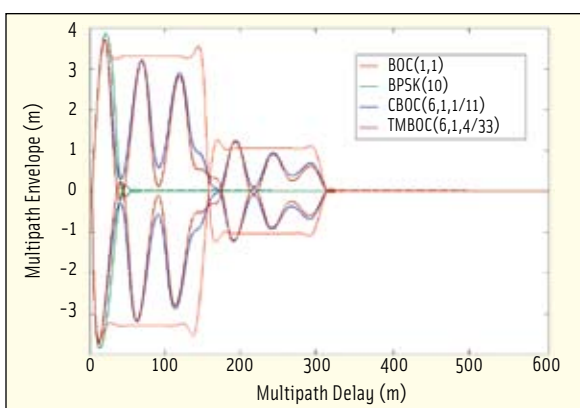FIGURE 7. Average Error for NELP Processing, BW=24 MHz (4 pole Butterworth filter), $\Delta\tau$=24.4 nsec

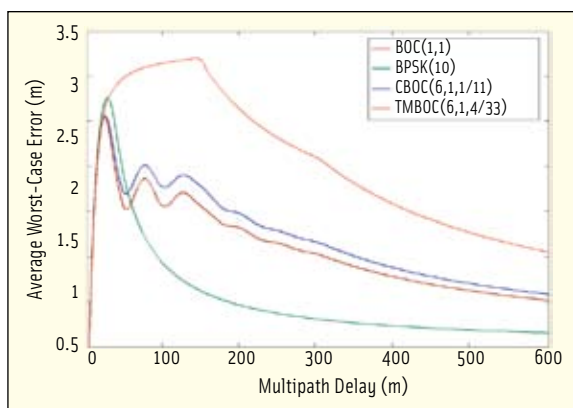FIGURE 8. Multipath Error Envelope for NELP Processing, W=24 MHz (6 pole Butterworth filter), d=0.0125 chips

FIGURE 9. Average Error for NELP Processing, BW=24 MHz (6 pole Butterworth filter), d=0.0125 chips

one direct and one reflected path, with a multipath to direct path signal power ratio (MDR) that is independent of delay. This model does not provide for the probability distribution of (reflected) path delay or the attenuation associated with each delay value.

The results shown here employ an MDR of –6 dB. The receiver is assumed to have a four- or six-pole Butterworth band-limiting filter with –3 dB points at the stated bandwidth (BW). The filter is assumed to be phase-equalized so that the group delay is constant. Non-coherent early-late processing (NELP) is employed.

The results are provided as pairs of graphs for each combination of receiver processing parameters and different signals. (Note that the scales of the figures vary and that some present the multipath delay in meters and others in nanoseconds, with 300 meters being approximately equal to 1000 nanosec-

onds.) The first graph is an error envelope showing maximum and minimum bias error (computed over all relative phases between the multipath and the direct path), for each delay. Many of these error envelopes have oscillatory components. The second graph is of the so-called running error. This is computed from the area enclosed within the multipath error envelope and averaged over the range of multipath delays from zero to the plotted delay values.

Figure 6 shows the multipath error envelope for the receiver configuration of most interest. It has a 24 MHz pre-correlation (double-sided) bandwidth and narrow early-late spacing of $\Delta\tau$=24.4 nsec, corresponding to a fraction d=0.025 of a 1.023 MHz spreading code chip period. **Figure 7** shows the corresponding running average error, revealing that both MBOC waveforms provide typically smaller average errors than either BOC(1,1) or BOC(2,2) waveforms.

One of the waveform options, TM or CBOC(6,1,4/33), shows an average error less than that of any other option for all delays. An important feature of all the MBOC waveforms is that the error envelope diminishes at smaller path length delay values than for BOC(1,1) or BOC(2,2). At longer path length delay values, the MBOC waveforms provide lower average delays similar in value to that of a BOC(2,2) spreading symbol.

Figure 8 and **Figure 9** show the corresponding results for 24 MHz precorrelation bandwidth, with a narrower early-late spacing $\Delta\tau$=12 ns, corresponding to d=0.0125 (proportion of a spreading code interval). In these figures, the multipath error envelope for a BPSK-R(10) spreading modulation has also been provided. Note that the MBOC spectrum provides error envelopes that are smaller than those for BPSK-R(10) for the small values of path length delays (less than ~120 ns). This is the range of delays that
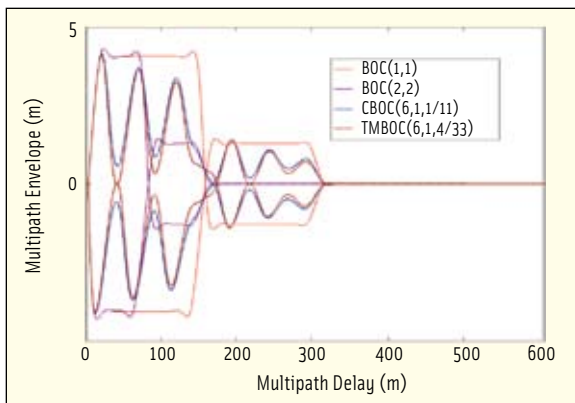
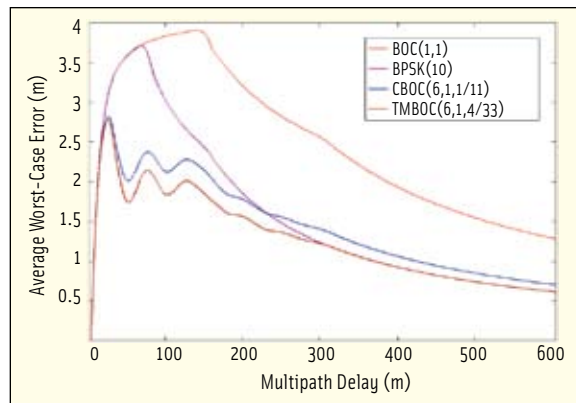FIGURE 10. Multipath Error Envelope for NELP Processing, BW=24 MHz (6 pole Butterworth filter), d=0.05 chips

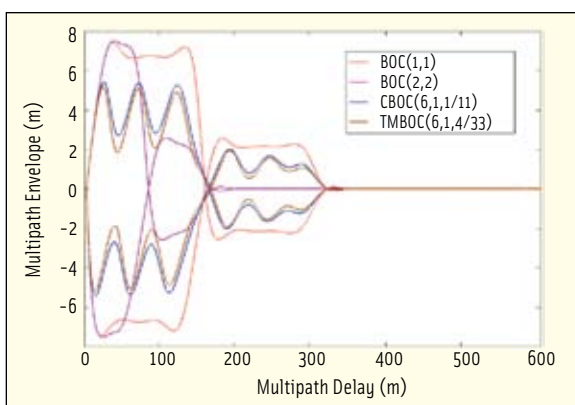FIGURE 11. Average Error for NELP Processing, BW=24 MHz (6 pole Butterworth filter), d=0.05 chips

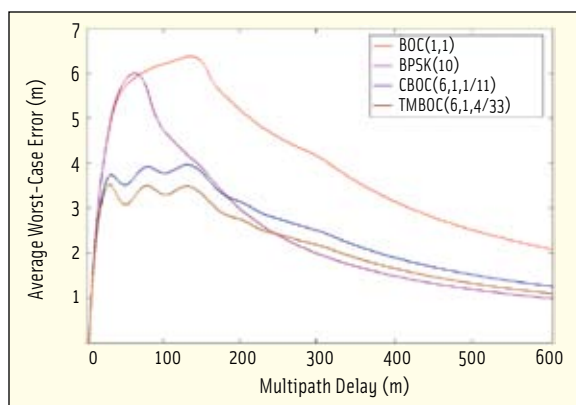FIGURE 12. Multipath Error Envelope for NELP Processing, BW=12 MHz (6 pole Butterworth filter), d=0.05 chips

FIGURE 13. Average Error for NELP Processing, BW=12 MHz (6 pole Butterworth filter), d=0.05 chips

are most common in many urban environments and have lower values of attenuation (typically less than 20-30 dB).

Figure 10 and **Figure 11** show results for BW=24 MHz, with early-late spacing of Δτ=48.9 nsec (d=0.05). The running average error of the MBOC waveforms are typically smaller than those for the BOC(1,1) or BOC(2,2) options. The error envelope for the MBOC(6,1,4/33) waveforms (TMBOC or CBOC) is smaller than for all other options.

Figure 12 and **Figure 13** show corresponding results for a narrower BW=12 MHz, with Δτ=48.9 nsec (d=0.05 chips). The average error of the CBOC and TMBOC waveform options are typically smaller than those for BOC(1,1) or BOC(2,2). The average errors for TMBOC(6,1,4/33) or CBOC(6,1,4/33) are smaller than those for any other choice for all multipath delays.

The results for narrow correlator processors show that TMBOC(6,1,4/33)

provides slightly smaller errors than for the CBOC(6,1,1/11) spreading symbol. This indicates that there is an advantage in placing all the BOC(6,1) spreading symbols in the pilot for certain applications. In every case examined, the average errors for TM - CBOC(6,1,4/33) and TM - CBOC(6,1,1/11) are smaller than those for BOC(2,2) for all delays.

Multipath Performance with Double-Delta Processing. Like early-late processing, double-delta multipath mitigation processing is a known processing technique that was designed for BPSK-R spreading modulations, but may be applied to more advanced modulations as well. The double-delta technique considered in this section processes every edge.

Smaller multipath error envelopes may be obtained from TMBOC and CBOC options by masking the BOC(6,1) spreading symbols in the receiver replica, so that only BOC(1,1) symbols are processed. This resulting code tracking SNR

after this masked symbol replica (MSR) processing, when compared to the code tracking SNR that would be obtained from an all BOC(1,1) pilot, would be a fraction of a dB lower (0.4, 0.6, or 0.9 dB, depending upon time series implementation). The difference in tracking error would be very small compared to other error sources, and all spreading symbols would be used for data demodulation and carrier tracking, thus making use of all the available power.

Figure 14 and **Figure 15** show the multipath errors resulting from double-delta processing with the same multipath propagation model used previously. In these figures, the BW=24 MHz, outer early-late spacing of 48.9 ns, and inner early-late spacing of 24.4 ns. With MSR processing, the multipath error envelopes for the MBOC options are the same as those for BOC(1,1), whilst those from BOC(2,2) are consistently larger. The multipath errors from double-delta
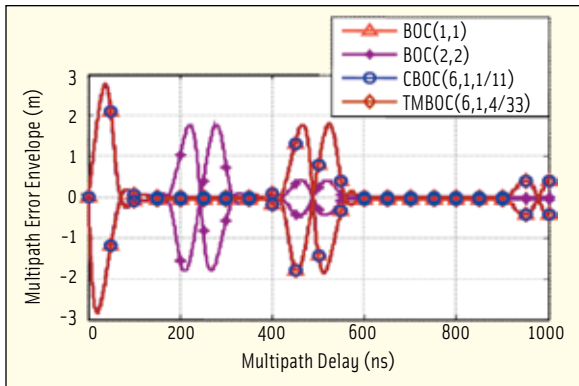
FIGURE 14. Multipath Error Envelope for Double–Delta Processing, BW=24 MHz (4 pole Butterworth filter), Early–Late Spacings of 24.4 nsec and 48.9 nsec
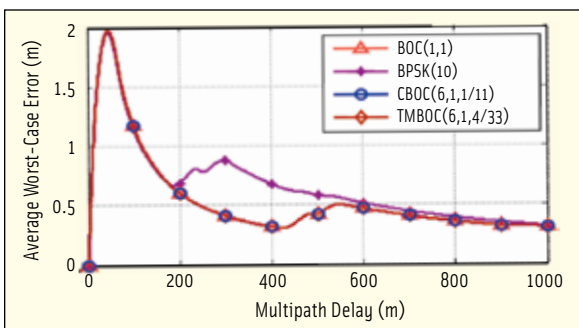

FIGURE 15. Average Error for Double–Delta Processing, BW=24 MHz (4 pole Butterworth filter), Early–Late Spacings of 24.4 nsec and 48.9 nsec
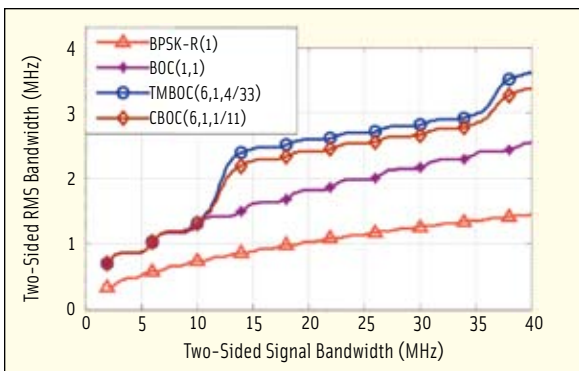

FIGURE 16. RMS bandwidth vs. two–sided receiver bandwidth

processing are much smaller than those from early-late processing.

Performance of Advanced Multipath Processing. A variety of advanced multipath mitigation techniques are evolving to provide improved performance. Further advances are expected to be possible with new forms of spreading modulations. No single metric provides for the comparison of signals for advanced mitigation techniques; therefore, we have considered two. The first of these is the

root-mean square (RMS) bandwidth of the spreading symbol, defined by

$$BW_{rms}(f_{\lim}) = \sqrt{\int_{-\frac{f_{\lim}}{2}}^{+\frac{f_{\lim}}{2}} f^2 \cdot \hat{G}(f) \cdot df} \quad \textbf{(9)}$$

where $\hat{G}(f)$ is normalized for unit power over the signal bandwidth being used, and $f_{\lim}$ is the double-sided receiver precorrelation bandwidth.

A brief note on this metric: In seeking to optimize a signal, researchers need a figure to minimize/maximize for comparison purposes, preferably one with a physical bound independent of the technique in receiver design. If not, the signal would only be optimized for certain receivers and not for others. The RMS bandwidth figure is related to the Cramer Rao lower bound and also the Gabor bandwidth; so, we considered it a good metric under certain constraints.

In the real world, of course, the number of multipath signals is unknown and can only be estimated. Additionally, the best estimator depends on the number of multipath signals, which increases the dimensionality and difficulty of the metrics problem.

Figure 15 shows the RMS bandwidth of the four spreading modulations for a given receiver bandwidth assumed to have rectangular bandwidths. The RMS bandwidths for the TMBOC and CBOC options are the same or larger than the RMS bandwidth for BOC(1,1) for all signal bandwidths, and larger or almost as large as those for BOC(2,2) for signal bandwidths greater than approximately 12 MHz. (High-performance receivers would be expected to use bandwidths

much greater than 12 MHz.)

As the results in **Figure 16** reflect, using a bandwidth of 12 MHz with one of the MBOC signal options would provide greater RMS bandwidth than using a 24 MHz bandwidth with BOC(1,1). If receivers use bandwidths less than approximately 12 MHz, they would lose a fraction of a dB of signal power with TMBOC or CBOC, compared to BOC(1,1).

A second measure of performance for advanced multipath mitigation is the number of waveform transitions in a code repeat interval. The more transitions the signal has, the better we can detect and remove multipath signals. In the case of MBOC this is exactly what is happening, because in both the TMBOC and CBOC implementations the BOC(6,1) component is oscillating at a higher frequency — or equally, there are more waveform transitions in a code repeat interval.

These are affected by the spreading symbol rate, the carrier offset frequency and the organization of the BOC(6,1) and BOC(1,1) components. A detailed analysis of this will not be given here. However, for the various options considered here, there is a gain of between 2.0 dB and 3.5 dB depending upon the specific waveform implementation used.

Summary of Multipath Performance. The multipath performance metrics indicate that early-late processing of TMBOC and CBOC options yields smaller multipath errors than the same processing of BOC(1,1). For the double-delta processor, the multipath errors for the proposed spreading symbol waveforms are the same as for BOC(1,1) and better than BOC(2,2). Both TMBOC and CBOC waveforms provide better potential for advanced multipath mitigation processing than BOC(1,1).

Spreading Code Performance

The new L1 Galileo OS and GPS L1C spreading code family members have been designed for reduced side-lobe levels in auto- and cross-correlation functions.

One of the metrics used to select the BOC(1,1) and BOC(6,1) spreading symbols as waveform partners is that these are orthogonal. (See the article by A. R. Pratt et al (2006) in the Additional Resources.") This can be used to improve the auto- and cross-correlation performance. Therefore, part of the design process for TMBOC implementations will be to select the locations in the code sequence where BOC(6,1) spreading symbols are placed. Judicious placement introduces zeros into the correlations at certain delays, providing a unique opportunity for additional control over the correlation functions.

The first results of this joint design of TMBOC placement and spreading codes has been completed for L1C. The pattern of BOC(6,1) spreading symbols is as shown in Figure 4. The sidelobe levels for crosscorrelations between L1C pilot codes, using the original codes selected for BOC(1,1) spreading modulations, and a different set of codes from the same family selected for TMBOC are shown in **Figure 17**.

The results are calculated using both even and odd crosscorrelations. Compared to the baseline spreading codes, the maximum crosscorrelation level is reduced by 0.1 dB, and its probability of occurrence is reduced by a factor of 40. The sidelobe levels at somewhat higher probability of occurrence are reduced by more than 1 dB. Similar improvements are evident in **Figure 18** for the autocorrelation sidelobes.

Performance of Low–End Receivers

GPS L1C and Galileo L1 OS signals are being designed to benefit receivers that will make use of technology advances to attain better performance, while continuing to support receivers designed for minimal complexity. For example, receivers that employ modest bandwidths and only use the BOC(1,1) spreading symbols may offer lower cost and provide long battery life.

The minimum double sided precorrelation bandwidth for a BOC(1,1) spreading symbol is approximately 4 MHz – about twice that required for

a C/A code receiver [BPSK-R(1)]. For maximum multipath mitigation performance, the widest precorrelation bandwidth provides the best performance. The BOC(6,1) component improves the signal to noise ratio for code tracking and multipath processing by up to 3.5 dB over BOC(1,1).

For intermediate receiver precorrelation bandwidths, the new signals continue to provide equal or better performance than BOC(1,1) signals and near those available from a BOC(2,2) spreading symbol. For low-end receivers with 4 MHz bandwidths, the MBOC options provide almost the same performance (within 0.4, 0.6, or 0.9 dB of power, depending upon spreading time series implementation), compared to BOC(1,1).

RF Compatibility

Since MBOC places more power at higher frequencies, it also provides some additional benefits in radio frequency compatibility. Compared to BOC(1,1), the MBOC(6,1,1/11) spectrum has 0.7 dB less self-interference, and 0.3 dB less interference to C/A code and SBAS receivers.

Summary and Way Ahead

This paper has described the optimized MBOC spreading modulation recommended for Galileo L1 OS and GPS L1C. The MBOC design continues the trend in most modernized signal designs to provide more power at higher frequencies (away from the center frequency) in order to improve code tracking and some aspects of multipath performance. MBOC does this by adding a small fraction of BOC(6,1) spectrum to the BOC(1,1) spectrum.

Since BOC(1,1) already has more high frequency power than C/A code's BPSK-R(1) spreading modulation, it already provides performance benefits over BPSK-R(1). MBOC provides additional benefits over BOC(1,1) including code tracking in noise and multipath (when using early-late processing and advanced multipath mitigation techniques). MBOC also produces better spreading code performance than the
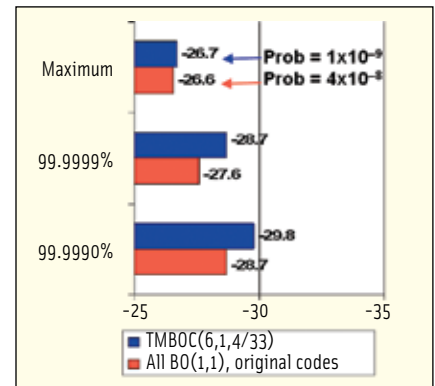
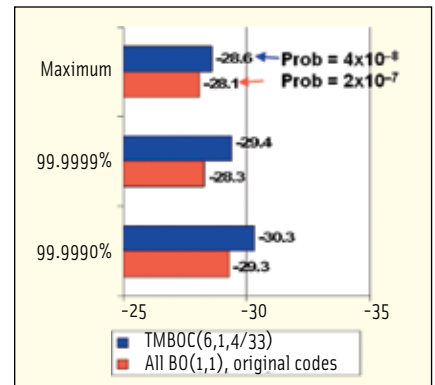FIGURE 17. **Comparison of Crosscorrelation Sidelobes for L1C**

FIGURE 18. **Comparison of Autocorrelation Sidelobes for L1C**

baseline L1C codes, less self-interference, better RF compatibility with C/A-code, and less susceptibility to narrowband interference at the worst-case frequency.

These improvements are obtained through the use of slightly more power at high frequencies. Receivers with very narrow front-end bandwidths do not obtain these benefits or use this signal power. Also, multipath mitigation techniques such as double-delta processing perform better with BPSK-R(1) than with MBOC or BOC(1,1) for receivers with narrower bandwidths. Thus, BPSK-R(1), BOC(1,1), and MBOC provide different opportunities to trade performance against support for simple receiver designs.

MBOC maintains compatibility with BOC(1,1) receivers, because more than 90 percent of the power remains available to BOC(1,1) receivers. Like BOC(1,1), MBOC provides good potential interoperability between GPS and Galileo, with greater interoperability

and compatibility achieved if the same time waveforms and spreading code families can be employed.

Several different waveform options exist and can produce the same MBOC(6,1,1/11) power spectral density, and evaluation of these different implementation options is continuing. The final choice between BOC(1,1) and MBOC as the common spreading modulation for L1 OS and L1C awaits an assessment of programmatic aspects for Galileo, with GPS prepared to proceed with either BOC(1,1) or MBOC.

Acknowledgments

References

[1] http://pnt.gov//public/docs/2004-US-EC-agreement.pdf

[2] http://gps.losangeles.af.mil/engineering/icwg/Docs/EC%20and%20US%20Joint%20Statement%20on%20GALILEO%20and%20GPS%20Signal%20Optimization%20-%20%2024%20Mar%202006.pdf

[3] http://gps.losangeles.af.mil/engineering/icwg/Docs/WGA%20Signed%20Recommendation%20on%20MBOC%20-%2023%20Mar%202006.pdf

[4] Avila-Rodriguez, J.A. et al. (2005), "Revised Combined Galileo/GPS Frequency and Signal Performance Analysis", **Proceedings of ION GNSS 2005** – 13-16 September 2005, Long Beach, California, USA.

[5] Betz, J. W., (2002), "Binary Offset Carrier Modulations for Radionavigation," **NAVIGATION: Journal of The Institute of Navigation** Vol. 48, No. 4, Winter 2001/02.

[6] Betz J. W. et al. (2002), "Candidate Design for an Additional Civil Signal in GPS Spectral Bands," **Proceedings of ION NTM 2002** - 28-30 January, 2002 - San Diego, CA

[7] Hegarty, C. J. et al. (2004), "Binary Coded Symbol Modulations for GNSS," **Proceedings of ION-AM-2004,** 7-9 June 2004, Dayton, Ohio, USA.

[8] Hein, G. W. et al. (2005), "A candidate for the GalileoL1 OS Optimized Signal", **Proceedings of ION GNSS 2005** – 13-16 September 2005, Long Beach, California, USA

[9] Pratt, A. R et al. (2003), "Performance of GPS Galileo Receivers Using m-PSK BOC Signals", **Proceedings of ION 2003** – 9-12 September 2003, Portland, Oregon, USA

[10] Pratt, A. R. et al. (2006), "Tracking Complex Modulation Waveforms – How to avoid Receiver Bias", **Proceedings of IEEE/ION PLANS 2006** – 24-27 April 2006, San Diego, California, USA.

[11] Wallner S. et al (2005), "Interference Computations between GPS and Galileo", **Proceedings of ION GNSS 2005** – 13-16 September 2005, Long Beach, California, USA

[12] Ries L. et al.(2003) "Tracking and Multipath performance Assessments of BOC Signals Using a Bit-Level Signal Processing Simulator", **Proceedings of ION 2003** - 9-12 September 2003 .Portland, Oregon, USA.

[13] Issler J.-L. et al. (2003) "Spectral measurements of GNSS satellite signals need for wide transmitted bands". **Proceedings of ION 2003** – 9-12 September 2003 .Portland, Oregon, USA.

Authors

"Working Papers" explore the technical and scientific themes that underpin GNSS programs and applications. This regular column is coordinated by **Prof. Dr.-Ing. Günter Hein**, a member of the European Commission's Galileo Signal Task Force and organizer of the annual Munich Satellite Navigation Summit. He has been a full professor and director of the Institute of Geodesy and Navigation at the University FAF Munich since 1983. In 2002, he received the United States Institute of Navigation Johannes Kepler Award for sustained and significant contributions to the development of satellite navigation. Hein received his Dipl.-Ing and Dr.-Ing. degrees in geodesy from the University of Darmstadt, Germany. Contact Professor Hein at <Guenter.Hein@unibw-muenchen.de>.

John W. Betz is a Fellow of The MITRE Corporation. He obtained a Ph.D. in electrical and computer engineering is from Northeastern University. Betz contributed to the design of the GPS M-code signal, led the Modulation and Acquisition Design Team, and developed the binary offset carrier (BOC) modulation. He has contributed to many aspects of GNSS engineering, and has participated in international efforts to achieve compatibility and interoperability between GPS and other satellite navigation systems. He received the ION Burka Award in 2001, and is a member of the US Air Force Scientific Advisory Board, and a Fellow of the Institute of Navigation (ION, U.S.).

José-Ángel Ávila-Rodríguez is research associate at the Institute of Geodesy and Navigation at the University of the Federal Armed Forces Munich. He is responsible for research activities on GNSS signals, including BOC, BCS, and MBCS modulations. He is involved in the Galileo program, in which he supports the European Space Agency, the European Commission, and the Galileo Joint Undertaking, through the Galileo Signal Task Force. He studied at the Technical Universities of Madrid, Spain, and Vienna, Austria, and has an M.S. in electrical engineering.

Christopher J. Hegarty is a senior principal engineer with The MITRE Corporation's Center for Advanced Aviation System Development. He received a D.Sc. in Electrical Engineering from The George Washington University. He is co-chair of the RTCA Inc. Special Committee 159. He was a recipient of the 1998 ION Early Achievement Award and the 2005 Johannes Kepler Award.

Stefan Wallner received his Diploma in Techno-Mathematics from the Technical University of Munichwith a and is now research associate at the Institute of Geodesy and Navigation at the University of the Federal Armed Forces Germany in Munich. His main topics of interests include the Galileo spreading codes and the signal structure.

Anthony R. Pratt graduated with a B.Sc. and Ph.D. in Electrical and Electronic Engineering from Birmingham University, United Kingdom. He joined the teaching staff at Loughborough University, UK in 1967 and remained until 1980. He has held several technical and managerial positions with private companies. He is also a Special Professor at the IESSG, University of Nottingham, UK. He acts as consultant to the UK Government in the development of Galileo Satellite System.

Lt. Lawrence S. Lenahan is the L1C Project Military Co-Chair and works for the NAVSTAR GPS Joint Program Office in its Engineering and Advanced Technology Branch, after three years with the 2d Space Operations Squadron as its engineer on-call for spacecraft anomalies. Lt. Lenahan received a B.S. degree from the United States Air Force Academy in astronautical engineering.

John I. R. Owen is the leader of navigation systems, Air Systems Department, UK Defence Science and Technology Laboratory (DSTL). He gained a BSc (Hons) in electrical and electronic engineering, Loughborough University, and joined the Royal Aircraft Establishment. He moved to the satellite navigation research group in 1982 and was responsible for the technical development of GPS receivers, antenna systems, and simulators in the UK. He is technical adviser to UK government departments for GPS and the European Galileo program, where he is active on the Signal Working Group, the Galileo Security Board and the European Space Agency Program Board for Navigation.

Jean-Luc Issler is head of the transmission techniques and signal processing department of CNES. With french ministries of transport and defense delegates, he represents France in the Galileo Signal Task Force of the European Commission.

Lionel Ries, Antoine DeLatour and Laurent Lestarquit, from his team, were involved in the design of CBOC, one of the recommended optimized Galileo OS signals. He is involved in the development of several spaceborne receivers in Europe. He received the "Astronautical Prize" from the "Association Aeronautique et Astronautique de France" for his involvement in the Galileo frequency choice and signal design.

Joseph J. Rushanan is a principal mathematician in the Signal Processing Section of the MITRE Corporation. His expertise includes discrete mathematics, including binary sequences, and general security engineering. He has a B.S. and M.S. from the Ohio State University and a Ph.D. from the California Institute of Technology, all in mathematics.

Andrea L. Kraay received a B.S. in electrical engineering from George Mason University, an S.M. and Engineer's degree in electrical engineering and computer science from the Massachusetts Institute of Technology and Woods Hole Oceanographic Institution. She is currently a senior engineer in the Signal Processing Group at the MITRE Corporation in Bedford, Massachusetts working in radar, navigation, and communications system design.

Tom Stansell heads Stansell Consulting, after eight8 years with the Johns Hopkins Applied Physics Laboratory, 25 years with Magnavox (Staff VP), and 5 years with Leica (VP), pioneering Transit and GPS navigation and survey products. He served on the WAAS Independent Review Board (2000); led technical development of the GPS L2C signal (2001); and is coordinator of the GPS L1C project. ION and other awards: Weems Award (1996), Fellow (1999), Kershner (PLANS-2000), GPS JPO Navstar Award (2002), and Johannes Kepler (2003). **IG**

InsideGNSS